Bioorganic Chemistry 87 (2019) 550–559

Contents lists available at ScienceDirect

Bioorganic Chemistry

journal homepage: www.elsevier.com/locate/bioorg

Synthesis, evaluation and docking of novel pyrazolo pyrimidines as potent p38α MAP kinase inhibitors with improved anti-inflammatory, ulcerogenic and TNF-α inhibitory properties

Kanagasabai Somakala, Sana Tariq, Mohd. Amir*

Department of Pharmaceutical Chemistry, School of Pharmaceutical Education and Research, Jamia Hamdard, New Delhi 110062, India

ARTICLE INFO

Keywords:
Pyrazolo pyrimidine
p38α MAP kinase
Docking
Anti-inflammatory
TNF-α inhibition

ABSTRACT

A series of nine new *N*-substituted-4-((1-phenyl-1*H*-pyrazolo[3,4-*d*]pyrimidin-4-yl)amino)benzamides (**6a-i**) derivatives was synthesized. All the compounds were screened *in-vitro* for BSA anti-denaturation property, antioxidant assay and p38α MAP kinase inhibition. The *in vitro* anti-inflammatory assay results revealed that the compounds (**6f-i**) showed better activity than the compounds **6a-e.** Compound **6f** bearing the 4-chlorophenyl group showed *in vitro* anti-inflammatory activity (82.35 ± 4.04) comparable to standard drug diclofenac sodium (84.13 ± 1.63) and better p38α MAP kinase inhibitory activity (IC_{50} = 0.032 ± 1.63 μM) than the prototypic inhibitor SB203580 (IC_{50} = 0.041 ± 1.75 μM). The selected active compounds (**6f-i**) were further studied in animal models for anti-inflammatory activity, ulcerogenic liability, lipid peroxidation and TNF-α inhibition potential. Compound **6f** showed promising anti-inflammatory potential with a percentage inhibition of 83.73% when compared to the standard, diclofenac sodium (78.05%). Compound **6f** was also found to show reduced ulcerogenic liability and lipid peroxidation in comparison to the standard. This compound also potently inhibited the lipopolysaccharide (LPS)-induced TNF-α production in mice model (ID_{50} = 8.23 mg/kg) in comparison to SB 203580 (ID_{50} = 26.38 mg/kg). The molecular docking of compounds **6a-i** against p38α MAP kinase receptor was also performed to understand ligand receptor interaction. Amongst all synthesized molecules compound **6f** displayed highest docking score of −9.824. It showed hydrogen bonding interactions with Asn115 and pi-cation interaction with Lys53.

1. Introduction

Non-steroidal anti-inflammatory drugs (NSAIDs) are considered one of the most useful clinical therapies for the treatment of pain, fever and inflammation [1]. The pharmacological activity of NSAIDs is related to the suppression of prostaglandin biosynthesis from arachidonic acid by inhibiting the enzyme Cyclooxygenases (COXs) and thromboxane synthase with a varying degree of selectivity [2]. It is well known that COX exists in two isoforms, COX-1 and COX-2, which are regulated differently [3]. COX-1 provides cytoprotection in the gastrointestinal (GI) tract whereas inducible COX-2 mediates inflammation [4]. Traditional non-steroidal anti-inflammatory drugs (NSAIDs) which inhibit both COX subtypes are still the most commonly used medications for inflammation and pain [5]. Diaryl heterocycles have become the major class of selective COX-2 inhibitors, such as celecoxib, rofecoxib, parecoxib and valdecoxib, which display improved gastrointestinal safety profile compared to the traditional NSAIDs [6–8]. NSAIDs acting through the inhibition of arachidonate metabolism are limited by toxicity and treat only the symptoms of pain and inflammation with no effect on the underlying disease process. Since the toxicity of NSAIDs is associated with their mechanism of action it may be difficult to separate efficacy from toxicity. The importance of inflammatory cytokines in the pathogenesis of inflammation has been demonstrated by the success of biologics in treating disease by blocking the effects of cytokines such as TNF-α, IL-1 or IL-6. Biological cytokine inhibitors, such as soluble TNF-α receptors (Etanercept), IL-1 receptor antagonists (Anakinra), or anti TNF antibodies (Infliximab, Adalimumab), are the new therapeutic strategies for treating inflammation [9,10]. However, limitations of these biologicals are adverse immunological reactions [9,11] and their high cost [12]. Also these existing regimens are effective in only a proportion of patients and crucially leave the host at significantly higher risk of overwhelming infection, e.g. tuberculosis, thus limiting their use in some populations. Therefore, new class of anti-inflammatory agents acting through novel mechanisms are needed which

* Corresponding author.
E-mail address: mamir_s2003@yahoo.co.in (M. Amir).

https://doi.org/10.1016/j.bioorg.2019.03.037
Received 6 December 2018; Received in revised form 6 March 2019; Accepted 14 March 2019
Available online 15 March 2019
0045-2068/

would treat the disease process as well as provide an alternative to the available biological cytokine inhibitors.

The development of orally active small molecule inhibitors to modify the proinflammatory cytokine release associated with inflammation represents an attractive alternative. p38 Mitogen-Activated Protein Kinase (MAPK) is a member of the intracellular family of MAP kinases implicated in the phosphorylation cascade leading to the release of TNF-α and other cytokines including interleukin-1beta (IL-1β), interleukin-6 (IL-6) and interleukin-8 (IL-8). p38 kinases are activated by a variety of stress stimuli including osmotic shock, ionizing radiation, mechanical wear, and cytokine stimulation [13]. Activation results in the release of TNF-α among other cytokines and the migration of white blood cells to the site of inflammation. p38 exists in four isoforms (α, β, γ, and δ) and expression of each isoform varies among different cell types of the immune system.

The p38α isoform is believed to be the most clinically relevant for the treatment of inflammation [14]. Hence, p38α has emerged as an attractive target for small molecule drug discovery to obstruct the action of TNF-α [15]. Pyrazolo[3,4-*d*]pyrimidine derivatives are such a class of heterocyclic compounds whose biological activities span a broad spectrum of antibacterial [16], antifungal [16], antiviral [17], anti-inflammatory [18,19], and anticancer [20–22] pharmacologies. Literature survey on pyrazolo[3,4-*d*]pyrimidines has shown that these derivatives also possess good p38α MAP kinase inhibition [23–26] (Fig. 1).

Encouraged by these observations and in continuation of our ongoing research program [26–32] to discover new and improved anti-inflammatory agents, we report herein the synthesis and pharmacological evaluation of pyrazolo[3,4-*d*]pyrimidine derivatives as potential anti-inflammatory agents.

2. Results and discussion

2.1. Chemistry

Nine pyrazolo [3,4-d] pyrimidine derivatives were synthesized by following the procedure mentioned under Scheme 1. Compounds **1–3** were synthesized according to the already reported procedures [19,33]. Phenyl hydrazine and ethoxymethylenemalononitrile were refluxed in ethanol to give the 4-cyano-5-amino derivative **1**. This cyano derivative was refluxed in formic acid to obtain the keto derivative **2** which was further converted to the chloro derivative **3** by treating with phosphorous oxychloride in few drops of DMF and refluxing the mixture. The chloro derivative was refluxed with ethyl-4-amino benzoate in ethanol to afford the ethyl acetate derivative **4** which on further treatment with 1N sodium hydroxide in THF-MeOH at room temperature gave the corresponding acid derivative (**5**). The acid derivative was refluxed with different amines (R/Ar-NH_2) in the presence of 1-ethyl-3-(3′-dimethyl amino) carbodiimide HCl salt (EDC), 1-hydroxy benzotriazole (HOBt), diisopropylethylamine in THF-DMF and ethanol to afford the final amide derivatives **6a-i**. The carbodiimide reacts with the carboxylic acid to form *O*-acyl isourea mixed anhydride. This intermediate then reacts with the amine to yield the desired amide and the urea by-product [34]. Furthermore, in this reaction, acetyl transfer may lead to the formation of the unreactive *N*-acyl urea. This side reaction was considerably diminished by the addition of nucleophile (HOBt) that reacts faster than the competing acyl transfer and generates an intermediate still active enough to couple with the amine and also

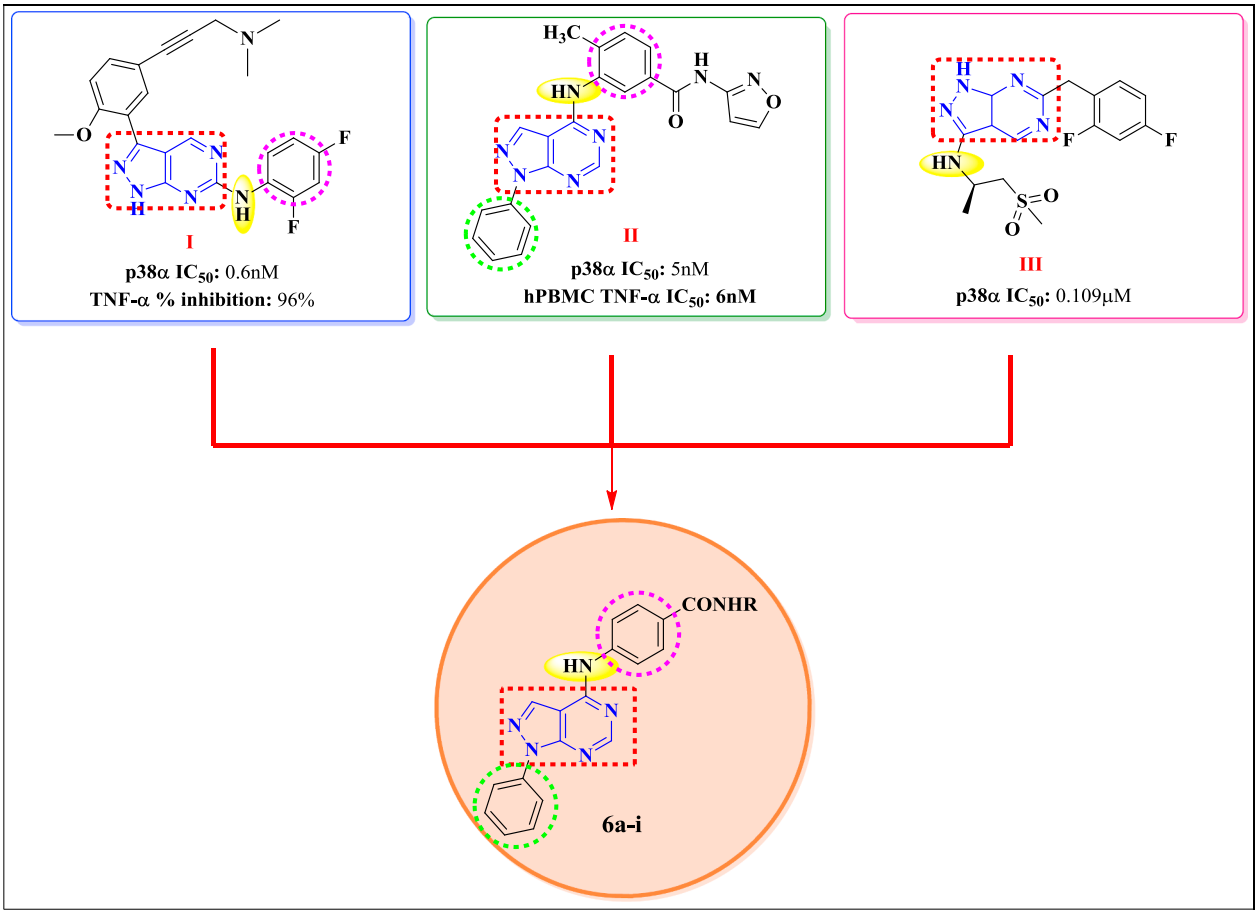

Fig. 1. Some previously reported pyrazolo[3,4-*d*]pyrimidine derivatives (**I** [18], **II** [19], **III** [20]) with their p38α and TNF-α inhibitory potentials and the designed compounds **6a-i**.

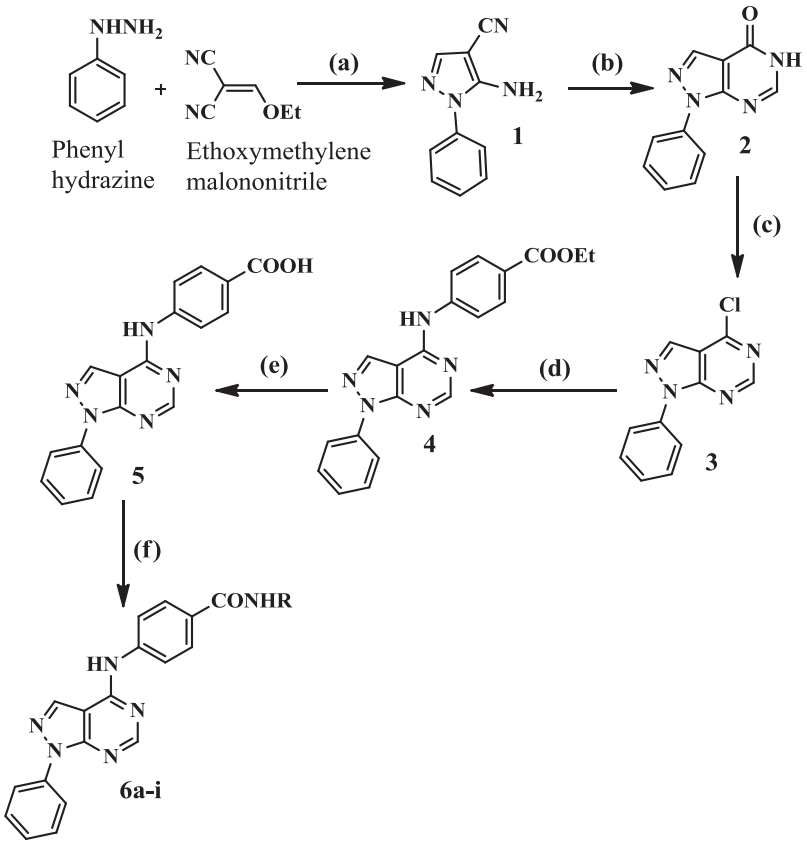

R= **a**: methyl, **b**: ethyl, **c**: n-propyl, **d**: isopropyl, **e**: n-butyl, **f**: 4-chlorophenyl, **g**: 4-fluorophenyl, **h**: 4-methylphenyl, **i**: 4-methoxyphenyl.

Scheme 1. (a) Ethanol, reflux; (b) Formic acid, reflux; (c) Phosphorous oxychloride, DMF, reflux; (d) Ethyl-4-amino benzoate, ethanol, reflux; (e) 1N NaOH, THF-MeOH, stir, rt; (f) EDC-HOBt, THF-DMF, R-NH_2, diisopropylethylamine, ethanol, reflux.

prevent the side reaction [35].

Compounds **1–3** were verified as already reported [19,33]. The ^{1}H NMR spectra of compound **4** showed a singlet at δ 10.50 ppm for NH proton. A quartet at δ 4.26 ppm corresponding to the CH_2 protons and a triplet at δ 1.31 ppm for CH_3 protons were also obtained showing the presence of an ethyl group. In the ^{1}H NMR spectra of compound **5**, the disappearance of the quartet and triplet for CH_2 and CH_3 protons and the appearance of a broad singlet at δ 12.71 ppm for the COOH proton confirmed the formation of compound **5**. The NH proton showed a singlet at δ 10.48 ppm. The ^{1}H NMR spectra of compounds **6a-i** showed a broad singlet at δ 11.38–11.15 ppm and a singlet at δ 10.52–10.13 ppm corresponding to the CONH and NH protons respectively. The two protons in the pyrazolo [3,4-d] pyrimidine nucleus showed singlets at δ 8.37–8.21 ppm and at δ 8.78–8.54 ppm. The CONH carbon in compounds **6a-i** showed a peak at δ 170.16–166.18 ppm in the ^{13}C NMR spectra. Mass spectra of compounds **6a-i** showed molecular ion peaks M^+ at an *m/z* corresponding to their molecular formula.

2.2. Biological evaluation

2.2.1. BSA in vitro assay

The BSA anti-denaturation screening of compounds **6a-i** showed that they exhibited activity in the range of 82.35–53.12% in comparison to diclofenac sodium which showed 84.13% inhibition. Compound **6f** (82.35%) showed the maximum anti-inflammatory activity. Compound **6i** (80.21%) also exhibited anti-inflammatory activity comparable to that of the standard drug. All other compounds showed activity in the range of 76.29–53.12% (Table 1).

2.2.2. Antioxidant in vitro assay

The maximum antioxidant potential was exhibited by compound **6f** (74.90%) when compared to BHA which showed 73.32% antioxidant activity. All the other synthesized compounds showed antioxidant activity ranging from 72.10 to 46.19% (Table 1).

2.2.3. p38α MAP kinase assay

Compounds **6a-i** were screened for their *in vitro* p38α MAPK inhibition. Compound **6f** possessing a 4-chlorophenyl group was found to exhibit the maximum p38α MAPK inhibition potential with an IC_{50} value of 0.032 ± 1.63 μM in comparison to the standard SB 203580 (IC_{50} = 0.041 ± 1.75 μM). Compound **6i** having a 4-methoxyphenyl group also showed a better inhibitory activity (IC_{50} = 0.038 ± 0.83 μM) in comparison to SB 203580. Compounds **6g** and **6h** having 4-fluorophenyl and 4-methylphenyl groups showed reduced p38α MAPK inhibition (IC_{50} = 0.185 ± 0.64 and 0.083 ± 1.25 μM respectively). Compounds **6a-e** possessing alkyl groups exhibited p38α MAPK inhibition ranging from 0.325 ± 1.12 to 1.321 ± 0.58 μM which was much lower than that of SB 203580 (Table 2).

2.2.4. Rat paw edema inhibition assay

Compounds **6f-i** which showed good *in vitro* activities, were further evaluated for the *in vivo* anti-inflammatory activity. The four tested compounds showed anti-inflammatory activity ranging from 70.58 to 83.73%, when compared to the standard drug, diclofenac sodium which showed 78.05% inhibition after 4 h. The most active compound in this series, **6f** with 83.73% inhibition possessed a 4-chloro phenyl group. Replacement of the 4-chloro phenyl group by a 4-methoxy phenyl

Table 1

In vitro anti-inflammatory activity (BSA denaturation inhibition assay) and % DPPH activity.

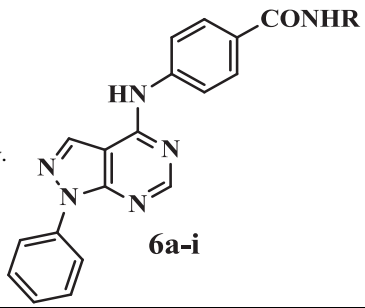

6a-i

Compounds	R	BSA Denaturation inhibition assay[a]		% DPPH activity (at 1 mM)[b]	
		Mean Absorbance	% Inhibition of denaturation ± SD*	Mean Absorbance	% antioxidant activity ± SD*
6a	Methyl	0.303	62.03 ± 4.57	0.354	56.93 ± 2.99
6b	Ethyl	0.286	53.12 ± 5.77	0.442	46.19 ± 1.09
6c	*n*-Propyl	0.288	54.01 ± 5.63	0.395	51.99 ± 0.81
6d	Isopropyl	0.293	56.51 ± 2.74	0.381	53.69 ± 1.09
6e	*n*-Butyl	0.307	64.17 ± 4.37	0.322	60.83 ± 1.58
6f	4-Chlorophenyl	0.341	82.35 ± 4.04	0.206	74.90 ± 2.72
6g	4-Fluorophenyl	0.323	72.55 ± 4.02	0.259	68.49 ± 5.34
6h	4-Methylphenyl	0.33	76.29 ± 3.22	0.242	70.60 ± 1.33
6i	4-Methoxyphenyl	0.337	80.21 ± 2.68	0.229	72.10 ± 3.53
Standard	–	0.344	84.13 ± 1.63	0.219	73.32 ± 0.74

* SD = Standard deviation (Average of three determinations).
[a] Diclofenac sodium.
[b] Butylated hydroxyl anisole.

Table 2
IC_{50} values against p38α MAP Kinase of **6a-i** and the standard, SB 203580.

Compounds	IC_{50} value (μM)[a]
6a	0.571 ± 0.36
6b	1.321 ± 0.58
6c	1.120 ± 1.47
6d	0.937 ± 0.78
6e	0.325 ± 1.12
6f	0.032 ± 1.63
6g	0.185 ± 0.64
6h	0.083 ± 1.25
6i	0.038 ± 0.83
SB 203580	0.041 ± 1.75

[a] Mean ± SEM of three experiments.

Table 3
Anti-inflammatory activity of **6f**, **6g**, **6h**, **6i** and diclofenac sodium.

Compounds	Increase in paw edema (ml) ± SEM (4 h)	% Inhibition	Activity relative to diclofenac sodium
6f	0.29 ± 0.042[c]	83.73	107.27
6g	0.52 ± 0.088[a]	70.58	90.43
6h	0.45 ± 0.059[a]	74.74	95.76
6i	0.42 ± 0.051[b]	76.35	97.82
Control	1.76 ± 0.062	–	–
Diclofenac sodium	0.39 ± 0.065	78.05	100

Anti-inflammatory activity of the compounds was compared with respect to control.
Data were analyzed by unpaired student's *t*-test for n = 6.
[a] $P < 0.05$.
[b] $P < 0.01$.
[c] $P < 0.001$.

group **6i** resulted in a decrease of activity (76.35%). Substitution with a 4-fluoro phenyl **6g** or a 4-methyl phenyl **6h** groups resulted in further decrease of anti-inflammatory activity (70.58 and 74.74% respectively) (Table 3).

2.2.5. Ulcerogenicity

The maximum reduction in ulcerogenic activity (0.250 ± 0.112) was found for compound **6f** having a 4-chloro phenyl group in comparison to the standard drug, diclofenac sodium which showed a high severity index of 1.667 ± 0.105. All the other derivatives showed moderate severity index ranging from 0.333 to 0.417 (Table 4).

2.2.6. Lipid peroxidation

The lipid peroxidation of compounds **6f**, **6g**, **6h** and **6i** were found to be in the range of 4.53 ± 0.309 to 5.78 ± 0.538 nmolMDA/100 mg when compared to the standard drug, diclofenac sodium (5.83 ± 0.063 nmolMDA/100 mg). The lipid peroxidation of compound **6f** was found to be less than that of diclofenac sodium, whereas compounds **6g**, **6h** and **6i** exhibited a similar lipid peroxidation to that of the standard (Table 4).

2.2.7. TNF-α inhibition assay

The inhibitory activity of derivatives **6f**, **6g**, **6h** and **6i** in the LPS-induced TNF-α production in mice were evaluated. Compound **6f** was found to be the most effective with an ID_{50} value of 8.23 mg/kg (and a % inhibition of 62.27). The ID_{50} value of the standard compound, SB 203580 was found to be 26.38 mg/kg and it exhibited an inhibition of 53.44%. The ID_{50} values of compounds **6h** and **6i** were found to be 13.64 and 11.79 mg/kg respectively. Compound **6g** was found to show the minimum TNF-α inhibitory potency of 57.17% (Table 4).

2.3. Docking studies

After *in-vitro* & *in-vivo* evaluation of compounds **6a-i** as anti-inflammatory agents they were docked against 2LGC.PDB ID to understand ligand receptor interaction. The PDB was prepared by protein preparation wizard of Maestro, the prepared protein was used for receptor grid generation, which was further validated.

2.3.1. Validation of docking protocol:

The validation is generally done by extracting the co-crystalized ligand and docking it again in the prepared grid. But, as the 2LGC.PDB ID did not contain any co-crystallized ligand, enrichment factor

Table 4
Ulcerogenic, lipid peroxidation and TNF- α inhibition activities of compounds (**6f-i)** and the standards.

Compounds	Mean severity index ± SEM	Lipid peroxidation nmolMDA/100 mg tissue	% TNF-α inhibition ± SEM	ID_{50} (mg/kg)
Control	0.00 ± 0.00	3.31 ± 0.113	–	–
6f	0.250 ± 0.112[a]	4.53 ± 0.309	62.27 ± 2.075[a]	8.23
6g	0.417 ± 0.154[c]	5.74 ± 0.691	57.17 ± 0.778[c]	–
6h	0.417 ± 0.083[c]	5.78 ± 0.538	58.27 ± 1.085[b]	13.64
6i	0.333 ± 0.167[a]	5.21 ± 0.291	60.07 ± 0.246[c]	11.79
Diclofenac sodium	1.667 ± 0.105	5.83 ± 0.063	–	–
SB 203580	–	–	53.44 ± 0.829	26.38

Data were analyzed by unpaired student's *t*-test for n = 6.
[a] P < 0.05.
[b] P < 0.01.
[c] P < 0.001.

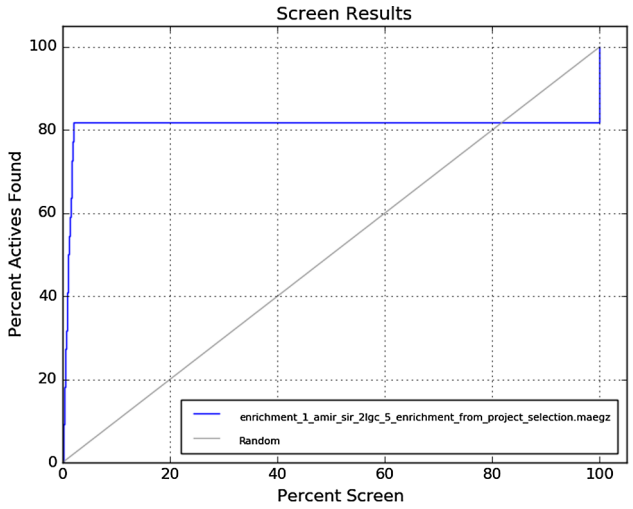

Fig. 2. ROC curve obtained after enrichment factor calculation for validation of docking protocol.

calculation was done to validate the docking protocol. A decoy dataset consisting of thousand molecules was merged with known active (22) p38α MAPK inhibitor. This dataset was prepared using ligprep and docked with the prepared grid of 2LGC.PDB ID. The docking protocol was able to separate known actives from decoy dataset and displayed a BEDROC of 0.949 (at alpha = 160.9, alpha*Ra = 3.4636); ROC of 0.82 and area under accumulation curve of 0.90 (Fig. 2), hence, docking protocol was validated and could be considered fit for conducting further docking studies.

2.3.2. Molecular docking:

Docking of prepared ligands (**6a-i**) was carried out on the prepared and validated grid on the Glide module of Maestro. Table 5 displays docking score (XP GScore) and predicted ADME properties (LogP o/w, PSA, LogS, Rule of five) of the compounds **6a-i**. The predicted Log P values are in compliance with Lipinski's rule of five. Polar surface area (PSA) is another important parameter used in estimating the drug transporter properties. PSA is the sum of surfaces of polar atoms such as oxygen, nitrogen and attached hydrogen and is vital for good oral bioavailability. The outcome of Lipinski's rule of five along with the other predicted parameters indicated that the compounds under consideration (**6a-i**) did elicit "drug-like" characteristics.

Amongst all synthesized molecules compound **6f** displayed highest docking score of −9.824. It showed hydrogen bonding interactions with Asn115 and pi-cation interaction with Lys53 (Figs. 3a and 3b), it also displayed good contacts with active site amino acids such as Leu75, Gly85, leu86, Leu 104, Val 105, Val 52, Lys 53, Ala 51, Val 38, Thr 106, Gly 36, His 107, Leu 108, Tyr 35, Gly 31, Gly 110, Val 30, Ala 51, Val 38, etc. (Fig. 3c) and bad contacts with amino acids: Val 30, Tyr 106, Ala 51, Lys 53 (Fig. 3d). The compound displayed no ugly interaction/contact.

Table 5
Docking score (XP GScore) and ADME properties (LogP o/w, PSA, LogS, Rule of five) of the synthesized compounds **6a-i.**

S. No.	Compound Name	Docking Score	LogP o/w[a]	PSA[b]	LogS[c]	Rule of five[d]
1.	**6a**	−9.074	3.365	85.714	−5.370	0
2.	**6b**	−8.992	3.807	84.650	−5.789	0
3.	**6c**	−9.824	4.166	84.611	−6.177	0
4.	**6d**	−8.784	4.196	83.402	−6.239	0
5.	**6e**	−8.900	4.539	84.604	−6.456	0
6.	**6f**	−9.824	4.806	82.482	−6.365	0
7.	**6g**	−8.592	4.756	82.482	−6.123	0
8.	**6h**	−8.980	4.899	82.482	−6.254	0
9.	**6i**	−7.595	4.785	90.650	−6.489	0
10.	SB 203580	−10.137	3.700	53.737	−4.409	0

[a] Predicted octanol/water partition coefficient (< 5).
[b] Van der Waals surface area of polar nitrogen and oxygen atoms and carbonyl carbon atoms (range 7–200).
[c] Predicted aqueous solubility, log S. S in mol dm–3 is the concentration of the solute in a saturated solution that is in equilibrium with the crystalline solid (Range - −6.5 to 0.5).
[d] Lipinski's violations (1).

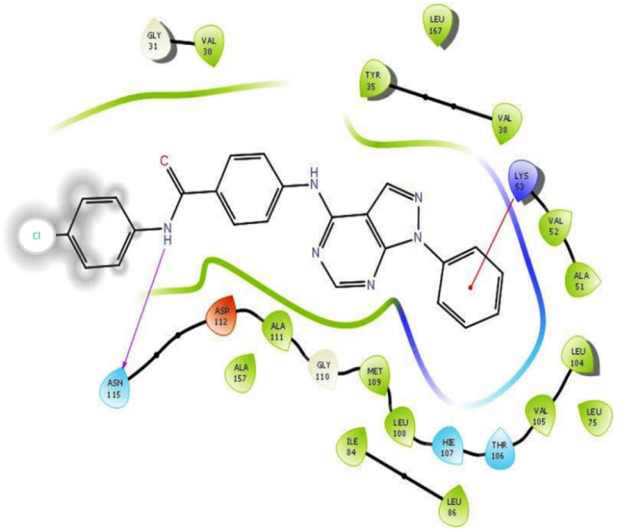

Fig. 3a. 2D Ligand Interaction diagram of **6f** in 2LGC.PDB ID.

3. Structure activity relationships

Nine pyrazolo [3,4-d] pyrimidine derivatives were synthesized and screened for *in vitro* anti-inflammatory, antioxidant and p38α MAP

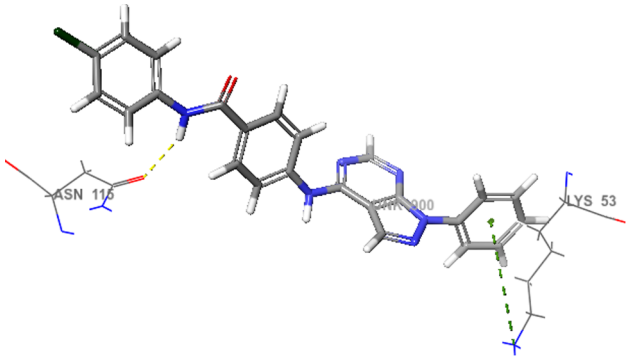

Fig. 3b. 3D interaction Ligand Interaction diagram of 6f with 2LGC.PDB ID (yellow: hydrogen bond; green: pi-cation bonding).

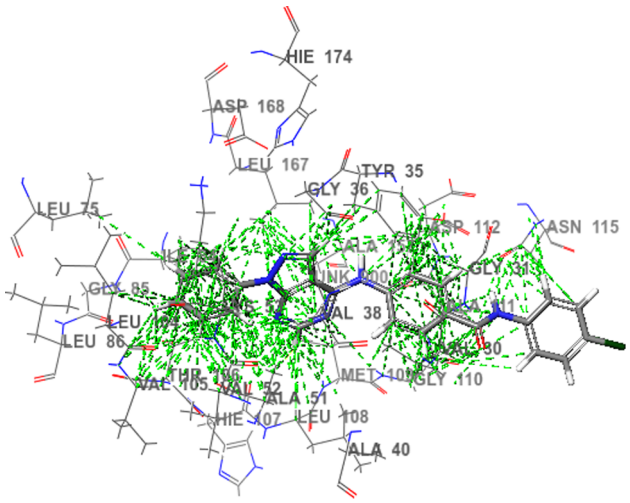

Fig. 3c. Good interactions/contacts of ligand **6f** with the active site amino acids of 2LGC.PDB ID.

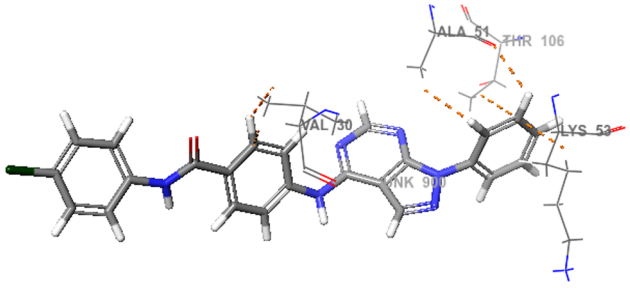

Fig. 3d. Bad interactions/contacts of ligand **6f** with the active site amino acids of 2LGC.PDB ID.

kinase inhibition activities. *In vitro* anti-inflammatory assay results showed that the compounds (**6f-i**) possessing 4-chloro phenyl (**6f**), 4-fluoro phenyl (**6g**), 4-methyl phenyl (**6h**) and 4-methoxy phenyl (**6i**) showed better activity than the compounds **6a-e** bearing alkyl groups (methyl **6a**, ethyl **6b**, *n*-propyl **6c**, isopropyl **6d** and *n*-butyl **6e**). From these results it is observed that the substituted phenyl groups present at the amide linkage of pyrazolo-pyrimidine moeity enhances the anti-inflammatory activity. Compound **6f** bearing the 4-chlorophenyl group showed *in vitro* anti-inflammatory activity (82.35 ± 4.04) comparable to standard drug diclofenac sodium (84.13 ± 1.63) and better p38α MAP kinase inhibitory activity (IC_{50} = 0.032 ± 1.63 μM) than the prototypic inhibitor SB203580 (IC_{50} = 0.041 ± 1.75 μM). Compounds **6f-i** which showed good *in vitro* potentials were further evaluated in animal models for their anti-inflammatory, ulcerogenic, lipid peroxidation and LPS-induced TNF-α production inhibition. It was found that compound **6f**, bearing the 4-chlorophenyl group at the amide linkage of the pyrazolo-pyrimidine ring showed higher anti-inflammatory activity (83.73%) than the standard drug diclofenac sodium (78.05%). The activity was decreased when the 4-chlorophenyl group was replaced by 4-methoxyphenyl (**6i**, 76.35%), 4-methylphenyl (**6h**, 74.74%) and 4-fluorophenyl groups (**6g**, 70.58%) respectively. It seems that compounds **6i** and **6h** having methoxy and methyl groups at the 4th position of phenyl ring are less active than **6f** due to their electron donating properties. Although compound **6g** having fluoro group at the 4th position of phenyl ring is electron withdrawing but showing reduced activity in comparison to **6f** which could be because of its high electronegativity and small size. This is further exemplified by its lower docking score (−8.592) in comparison to **6f** (−9.824). It was found that compound **6f** showing high anti-inflammatory activity also exhibited reduced ulcerogenic potential. Furthermore, this compound showed reduced lipid peroxidation and also demonstrated good inhibition of TNF-α production in mice. It was observed from the above studies that compounds showing significant *in vitro* p38α MAP kinase activity also showed good *in vivo* anti-inflammatory activity. Furthermore, molecular docking study of compound **6f** revealed favorable orientation within the active binding site of p38α MAP kinase having a docking score comparable with prototype p38α MAP kinase inhibitor SB 203580. In conclusion, this preliminary investigation showed that compound **6f** can serve as a promising scaffold in search for new and safer anti-inflammatory agents.

4. Experimental section

4.1. Chemistry

The reagents and solvents used were of laboratory grade and were procured from Merck (Darmstadt, Germany) and S.D. Fine chemicals (Delhi, India). Melting points (°C) were recorded using a Labtronics digital melting point apparatus (Haryana, India) and were uncorrected. IR spectra (KBr) were recorded on a Perkin-Elmer 1720 FTIR spectrometer (ν in cm^{-1}) (New York, USA). ^{1}H NMR spectra (400 MHz) and ^{13}C NMR spectra (100 MHz) were obtained on a Bruker Avance NMR spectrometer (Zurich, Switzerland) using Tetramethysilane (TMS) as the internal reference (chemical shifts in δ). MS analyses were performed on a Jeol SX-102 spectrometer (Tokyo, Japan). Thin layer chromatography (TLC) was performed on silica gel G (Merck) and spots were visualized under the ultraviolet light (UV: 254 nm). Elemental analyses (C, H and N) were conducted using a CHNS Vario EL III machine (Elementar Analysen systeme GmbH, Germany) and the results are within 0.4% of theoretical value.

4.1.1. Synthesis of 5-amino-1-phenyl-1H-pyrazole-4-carbonitrile 1

Phenyl hydrazine (0.01 mol) was added to absolute ethanol (30 mL). To this solution ethoxymethylenemalononitrile (0.01 mol) was added dropwise with stirring at room temperature. The resultant solution was refluxed for 1 h. The reaction mixture was set aside overnight to obtain the solid. The compound was purified by recrystallization from ethanol.

White crystals; yield 96%; m.p. 140–142 °C; IR: (KBr, cm^{-1}): 3412, 3308 (NH_2), 1593 (C=C), 1542 (C=N), 2238 (C≡N); ^{1}H NMR (400 MHz, $CDCl_3$): δ = 4.61 (s, 2H, NH_2, D_2O exchangeable), 7.43–7.55 (m, 5H, ArH), 7.65 (s, 1H, ArH).

4.1.2. Synthesis of 1-phenyl-1H-pyrazolo[3,4-d]pyrimidin-4(5H)-one 2

5-Amino-1-phenyl-1*H*-pyrazole-4-carbonitrile **1** (0.01 mol) was refluxed in formic acid (50 mL) for **6h**. The reaction mixture was then cooled and poured into crushed ice. The precipitate thus obtained was filtered, dried and recrystallized from ethanol.

White powder; yield 91%; m.p. 265–267 °C; IR (KBr, cm^{-1}): 3428 (NH), 1678 (C=O), 1588 (C=C), 1539 (C=N); ^{1}H NMR (400 MHz, DMSO-d_6): δ = 7.50 (t, 1H, ArH, J = 7.6 Hz), 7.66 (t, 2H, ArH,

J = 7.6 Hz), 8.13 (d, 2H, ArH, J = 8 Hz), 8.29 (s, 1H, ArH), 8.43 (s, 1H, ArH), 12.51 (brs, 1H, NH, D_2O exchangeable).

*4.1.3. Synthesis of 4-chloro-1-phenyl-4,5-dihydro-1H-pyrazolo[3,4-d] pyrimidine **3***

Phosphorous oxychloride (15 mL) containing few drops of DMF was added dropwise to 1-phenyl-1*H*-pyrazolo[3,4-*d*]pyrimidin-4(5*H*)-one (0.01 mol) with stirring at room temperature. The mixture was refluxed for 2 h, cooled to room temperature and then poured into crushed ice with vigorous stirring. The resultant precipitate was filtered, dried and recrystallized from ethanol.

Yellow crystals; yield 91%; m.p. 199–200 °C; IR (KBr, cm^{-1}): 1612 (C═C), 1535 (C═N), 742 (C−Cl); ^{1}H NMR (400 MHz, DMSO-d_6): δ = 7.38 (t, 1H, ArH, J = 7.6 Hz), 7.54 (t, 2H, ArH, J = 7.6 Hz), 8.01 (d, 2H, ArH, J = 7.6 Hz), 8.18 (s, 1H, ArH), 8.31 (s, 1H, ArH).

*4.1.4. Synthesis of ethyl 4-((1-phenyl-4,5-dihydro-1H-pyrazolo[3,4-d] pyrimidin-4-yl)amino)benzoate **4***

A mixture of compound **3** (0.01 mol) and ethyl-4-amino benzoate (0.01 mol) in the presence of absolute ethanol (50 mL) was refluxed for 2 h. The reaction mixture was then cooled to room temperature and poured into crushed ice to get ethyl 4-((1-phenyl-4,5-dihydro-1*H*-pyrazolo[3,4-*d*]pyrimidin-4-yl)amino)benzoate which was further dried and recrystallized from ethanol.

White crystals; yield 86%; m.p. 156–158 °C; IR (KBr, cm^{-1}): 3325 (NH), 1718 (C═O), 1589 (C═C), 1558 (C═N); ^{1}H NMR (400 MHz, DMSO-d_6): δ 1.31 (t, 3H, CH_3, J = 7.2 Hz), 4.26 (q, 2H, CH_2, J = 7.2 Hz), 7.38 (t, 1H, ArH, J = 7.6 Hz), 7.56 (t, 2H, ArH, J = 7.6 Hz), 7.98 (d, 2H, ArH, J = 8.4 Hz), 8.07 (d, 2H, ArH, J = 8.8 Hz), 8.18 (d, 2H, ArH, J = 8 Hz), 8.63 (s, 1H, ArH), 8.65 (s, 1H, ArH), 10.50 (s, 1H, NH, D_2O exchangeable).

*4.1.5. Synthesis of 4-((1-phenyl-4,5-dihydro-1H-pyrazolo[3,4-d] pyrimidin-4-yl)amino)benzoic acid **5***

The ester **4** (0.01 mol) was stirred at room temperature with 1 N aqueous NaOH (10 mL) in the presence of THF-MeOH (1:1, 30 mL). The reaction mixture was then poured into crushed ice and the precipitate thus obtained was filtered, dried and recrystallized from ethanol.

White powder; yield 82%; m.p. 143–145 °C; IR (KBr, cm^{-1}): 3352 (NH), 3264, 1716 (COOH), 1611 (C═C), 1578 (C═N); ^{1}H NMR (400 MHz, DMSO-d_6): δ 7.36 (t, 1H, ArH, J = 7.6 Hz), 7.55 (t, 2H, ArH, J = 7.6 Hz), 7.96–8.06 (m, 4H, ArH), 8.18 (d, 2H, ArH, J = 8 Hz), 8.61 (s, 1H, ArH), 8.65 (s, 1H, ArH), 10.48 (s, 1H, NH), 12.71 (s, 1H, COOH).

*4.1.6. General method for the synthesis of N-substituted-4-((1-phenyl-1H-pyrazolo[3,4-d]pyrimidin-4-yl)amino)benzamides **6a-i***

To a solution of **5** (0.005 mol) in THF-DMF (20 mL), diisopropylethylamine (0.097 mol) was added. The mixture was then treated with EDC-HCl (0.0005 mol), HOBt (0.0005 mol) and different amines (0.005 mol). The reaction mixtures were refluxed for 6–8 h, cooled and then poured into ice cold water. The resultant mixtures were extracted with ethylacetate and the extracts were concentrated and kept aside overnight to obtain the solids. The compounds thus obtained were filtered, dried and recrystallized from ethanol.

*4.1.6.1. N-Methyl-4-((1-phenyl-1H-pyrazolo[3,4-d]pyrimidin-4-yl) amino) Benzamide (**6a**).* White crystals; yield 88%; m.p. 265–267 °C; IR (KBr, cm^{-1}): 3413 (NH), 1688 (CONH), 1588 (C═C), 1558 (C═N); ^{1}H NMR (400 MHz, DMSO-d_6): δ = 2.80 (s, 3H, CH_3), 7.43 (t, 1H, ArH, J = 7.6 Hz), 7.52 (t, 2H, ArH, J = 7.6 Hz), 7.88–7.72 (m, 4H, ArH), 7.89 (d, 2H, ArH, J = 8 Hz), 8.32 (s, 1H, ArH, pyrazole), 8.65 (s, 1H, ArH, pyrimidine), 10.35 (s, 1H, NH), 11.29 (s, 1H, CONH); ^{13}C NMR (100 MHz, DMSO-d_6): δ = 27.96 (CH_3), 121.25, 122.37, 123.59, 125.15, 128.48, 128.63, 128.72, 128.93, 130.17, 130.46, 134.70, 136.45, 136.92, 167.21 (CONH); ESI-MS (m/z): 345 $[M + H]^+$; Anal. Calcd. for $C_{19}H_{16}N_6O$: C, 66.27; H, 4.68; N, 24.40%. Found: C, 66.19; H, 4.62; N, 24.47%.

*4.1.6.2. N-Ethyl-4-((1-phenyl-1H-pyrazolo[3,4-d]pyrimidin-4-yl)amino) Benzamide (**6b**).* White crystals; yield 86%; m.p. 230–232 °C; IR (KBr, cm^{-1}): 3421 (NH), 1667 (CONH), 1590 (C═C), 1553 (C═N); ^{1}H NMR (400 MHz, DMSO-d_6): δ = 1.56 (t, 3H, CH_3, J = 7.2 Hz), 3.32 (q, 2H, CH_2, J = 7.2 Hz), 7.45 (t, 1H, ArH, J = 7.6 Hz), 7.59 (t, 2H, ArH, J = 7.6 Hz), 7.68–7.75 (m, 4H, ArH), 7.81 (d, 2H, ArH, J = 8 Hz), 8.11 (s, 1H, ArH, pyrazole), 8.28 (s, 1H, ArH, pyrimidine), 10.49 (s, 1H, NH), 11.56 (s, 1H, CONH); ^{13}C NMR (100 MHz, DMSO-d_6): δ = 16.52 (CH_3), 33.96 (CH_2), 120.85, 122.53, 123.77, 126.71, 127.38, 128.32, 128.54, 128.82, 130.11, 130.40, 133.45, 136.79, 137.52, 168.52 (CONH); ESI-MS (m/z): 359 $[M + H]^+$; Anal. Calcd. for $C_{20}H_{18}N_6O$: C, 67.02; H, 5.06; N, 23.45%. Found: C, 67.11; H, 5.13; N, 23.48%.

*4.1.6.3. N-Propyl-4-((1-phenyl-1H-pyrazolo[3,4-d]pyrimidin-4-yl)amino) Benzamide (**6c**).* Light yellow crystals; yield 70%; m.p. 260–261 °C; IR (KBr, cm^{-1}): 3417 (NH), 1684 (CONH), 1574 (C═C), 1562 (C═N); ^{1}H NMR (400 MHz, DMSO-d_6): δ = 1.02 (t, 3H, CH_3, J = 7.2 Hz), 3.52 (t, 2H, CH_2, J = 7.2 Hz), 3.30–3.46 (m, 2H, CH_2), 7.43 (t, 1H, ArH, J = 7.6 Hz), 7.58 (t, 2H, ArH, J = 7.6 Hz), 7.67–7.73 (m, 4H, ArH), 7.80 (d, 2H, ArH, J = 8 Hz), 8.28 (s, 1H, ArH, pyrazole), 8.65 (s, 1H, ArH, pyrimidine), 10.23 (s, 1H, NH), 11.31 (s, 1H, CONH); ^{13}C NMR (100 MHz, DMSO-d_6): δ = 12.33 (CH_3), 25.21 (CH_2), 41.92 (CH_2), 119.54, 120.52, 122.41, 123.57, 125.78, 127.73, 128.68, 128.91, 129.64, 130.37, 130.81, 133.78, 136.15, 170.16 (CONH); ESI-MS (m/z): 373 $[M + H]^+$; Anal. Calcd. for $C_{21}H_{20}N_6O$: C, 67.73; H, 5.41; N, 22.57%. Found: C, 67.68; H, 5.49; N, 22.53%.

*4.1.6.4. N-Isopropyl-4-((1-phenyl-1H-pyrazolo[3,4-d]pyrimidin-4-yl) amino) Benzamide (**6d**).* White crystals; yield 85%; m.p. 265–267 °C; IR (KBr, cm^{-1}): 3430 (NH), 1693 (CONH), 1582 (C═C), 1543 (C═N); ^{1}H NMR (400 MHz, DMSO-d_6): δ = 1.26 (d, 6H, $(CH_3)_2$, J = 6 Hz), 4.06–3.99 (m, 1H, CH), 7.45 (t, 1H, ArH, J = 7.6 Hz), 7.61 (t, 2H, ArH, J = 7.6 Hz), 7.78–7.83 (m, 4H, ArH), 7.94 (d, 2H, ArH, J = 8 Hz), 8.27 (s, 1H, ArH, pyrazole), 8.59 (s, 1H, ArH, pyrimidine), 10.25 (s, 1H, NH), 11.15 (s, 1H, CONH); ^{13}C NMR (100 MHz, DMSO-d_6): δ = 12.33 (CH_3), 22.98 ($(CH_3)_2$), 47.15 (CH), 119.87, 121.25, 122.36, 123.55, 125.17, 128.48, 128.72, 128.78, 128.93, 130.16, 130.47, 134.70, 136.45, 166.71 (CONH); ESI-MS (m/z): 373 $[M + H]^+$; Anal. Calcd. for $C_{21}H_{20}N_6O$: C, 67.73; H, 5.41; N, 22.57%. Found: C, 67.65; H, 5.52; N, 22.52%.

*4.1.6.5. N-Butyl-4-((1-phenyl-1H-pyrazolo[3,4-d]pyrimidin-4-yl)amino) Benzamide (**6e**).* Light yellow crystals; yield 89%; m.p. 251–252 °C; IR (KBr, cm^{-1}): 3428 (NH), 1662 (CONH), 1595 (C═C), 1539 (C═N); ^{1}H NMR (400 MHz, DMSO-d_6): δ = 1.06 (t, 3H, CH_3, J = 7.6 Hz), 1.36–1.29 (m, 2H, CH_2), 1.59–1.50 (m, 2H, CH_2), 3.35 (t, 2H, CH_2, J = 7.6 Hz), 7.50 (t, 1H, ArH, J = 7.6 Hz), 7.56 (t, 2H, ArH, J = 7.6 Hz), 7.68–7.84 (m, 4H, ArH), 7.92 (d, 2H, ArH, J = 8 Hz), 8.32 (s, 1H, ArH, pyrazole), 8.65 (s, 1H, ArH, pyrimidine), 10.32 (s, 1H, NH), 11.21 (s, 1H, CONH); ^{13}C NMR (100 MHz, DMSO-d_6): δ = 14.23 (CH_3), 20.07 (CH_2), 32.96 (CH_2), 38.94 (CH_2), 118.96, 120.85, 122.57, 123.79, 126.71, 127.33, 128.28, 128.52, 128.83, 130.11, 130.45, 133.50, 136.74, 168.23 (CONH); ESI-MS (m/z): 387 $[M + H]^+$; Anal. Calcd. for $C_{22}H_{22}N_6O$: C, 68.38; H, 5.74; N, 21.75%. Found: C, 68.45; H, 5.66; N, 21.70%.

*4.1.6.6. N-(4-Chlorophenyl)-4-((1-phenyl-1H-pyrazolo[3,4-d]pyrimidin-4-yl)amino) Benzamide (**6f**).* White crystals; yield 86%; m.p. 282–283 °C; IR (KBr, cm^{-1}): 3387 (NH), 1695 (CONH), 1584 (C═C), 1541 (C═N); ^{1}H NMR (400 MHz, DMSO-d_6): δ = 7.39 (t, 1H, ArH, J = 7.6 Hz), 7.45 (d, 2H, ArH, J = 7.6 Hz), 7.52 (t, 2H, ArH, J = 7.6 Hz), 7.61 (d, 2H, ArH, J = 7.6 Hz), 7.64–7.72 (m, 4H, ArH), 7.84 (d, 2H, ArH, J = 8 Hz), 8.37 (s, 1H, ArH, pyrazole), 8.54 (s, 1H, ArH, pyrimidine), 10.13 (s, 1H, NH), 11.31 (s, 1H, CONH); ^{13}C NMR

(100 MHz, DMSO-d_6): δ = 118.82, 120.97, 122.05, 123.53, 125.24, 128.07, 128.41, 128.56, 128.59, 129.08, 129.33, 134.76, 135.07, 135.86, 137.51, 143.95, 152.53, 167.96 (CONH); ESI-MS (*m/z*): 441 $[M+H]^+$, 442 $[M+2]^+$; Anal. Calcd. for $C_{24}H_{17}ClN_6O$: C, 65.38; H, 3.89; N, 19.06%. Found: C, 65.47; H, 3.80; N, 19.01%.

4.1.6.7. N-(4-Bromophenyl)-4-((1-phenyl-1H-pyrazolo[3,4-d]pyrimidin-4-yl)amino) Benzamide ***(6g)***. Yellow crystals; yield 83%; m.p. 258–259 °C; IR (KBr, cm^{-1}): 3395 (NH), 1681 (CONH), 1591 (C═C), 1558 (C═N); ^{1}H NMR (400 MHz, DMSO-d_6): δ = 7.32 (t, 1H, ArH, J = 7.6 Hz), 7.41 (d, 2H, ArH, J = 7.6 Hz), 7.58 (t, 2H, ArH, J = 7.6 Hz), 7.63 (d, 2H, ArH, J = 7.6 Hz), 7.72–7.81 (m, 4H, ArH), 7.97 (d, 2H, ArH, J = 8 Hz), 8.24 (s, 1H, ArH, pyrazole), 8.58 (s, 1H, ArH, pyrimidine), 10.52 (s, 1H, NH), 11.38 (s, 1H, CONH); ^{13}C NMR (100 MHz, DMSO-d_6): δ = 116.75, 119.53, 120.61, 122.35, 123.52, 125.74, 127.69, 128.74, 128.91, 129.67, 130.28, 130.87, 133.85, 136.20, 137.48, 139.08, 142.56, 168.01 (CONH); ESI-MS (*m/z*): 486 $[M+H]^+$, 487 $[M+2]^+$; Anal. Calcd. for $C_{24}H_{17}BrN_6O$: C, 59.39; H, 3.53; N, 17.32%. Found: C, 59.47; H, 3.44; N, 17.38%.

4.1.6.8. N-(4-Methylphenyl)-4-((1-phenyl-1H-pyrazolo[3,4-d]pyrimidin-4-yl)amino) Benzamide ***(6 h)***. White crystals; yield 75%; m.p. 221–222 °C; IR (KBr, cm^{-1}): 3422 (NH), 1675 (CONH), 1577 (C═C), 1533 (C═N); ^{1}H NMR (400 MHz, DMSO-d_6): δ = 2.23 (s, 3H, CH_3), 7.39 (t, 1H, ArH, J = 7.6 Hz), 7.46 (d, 2H, ArH, J = 7.6 Hz), 7.53 (t, 2H, ArH, J = 7.6 Hz), 7.64 (d, 2H, ArH, J = 7.6 Hz), 7.65–7.72 (m, 4H, ArH), 7.80 (d, 2H, ArH, J = 8 Hz), 8.25 (s, 1H, ArH, pyrazole), 8.57 (s, 1H, ArH, pyrimidine), 10.13 (s, 1H, NH), 11.19 (s, 1H, CONH); ^{13}C NMR (100 MHz, DMSO-d_6): δ = 18.32 (CH_3), 118.81, 120.93, 122.12, 123.46, 125.39, 128.05, 128.34, 128.52, 128.57, 129.08, 129.37, 134.71, 135.03, 135.86, 137.51, 143.97, 152.53, 166.29 (CONH); ESI-MS (*m/z*): 421 $[M+H]^+$. Anal. Calcd. for $C_{25}H_{20}N_6O$: C, 71.41; H, 4.79; N, 19.99%. Found: C, 71.50; H, 4.72; N, 19.93%.

4.1.6.9. N-(4-Methoxyphenyl)-4-((1-phenyl-1H-pyrazolo[3,4-d] pyrimidin-4-yl)amino) Benzamide ***(6i)***. White powder; yield 80%; m.p. 276–277 °C; IR (KBr, cm^{-1}): 3426 (NH), 1672 (CONH), 1582 (C═C), 1556 (C═N); ^{1}H NMR (400 MHz, DMSO-d_6): δ = 3.74 (s, 3H, OCH_3), 7.38 (t, 1H, ArH, J = 7.6 Hz), 7.47 (d, 2H, ArH, J = 7.6 Hz), 7.59 (t, 2H, ArH, J = 7.6 Hz), 7.68 (d, 2H, ArH, J = 7.6 Hz), 7.70–7.82 (m, 4H, ArH), 7.93 (d, 2H, ArH, J = 8 Hz), 8.21 (s, 1H, ArH, pyrazole), 8.78 (s, 1H, ArH, pyrimidine), 10.33 (s, 1H, NH), 11.30 (s, 1H, CONH); ^{13}C NMR (100 MHz, DMSO-d_6): δ = 57.62 (OCH_3), 118.75, 119.81, 121.29, 122.33, 123.50, 125.18, 128.47, 128.63, 128.68, 128.93, 130.21, 130.48, 134.75, 136.47, 136.90, 138.28, 144.62, 166.18 (CONH); ESI-MS (*m/z*): 437 $[M+H]^+$; Anal. Calcd. for $C_{25}H_{20}N_6O_2$: C, 68.80; H, 4.62; N, 19.25%. Found: C, 68.86; H, 4.53; N, 19.22%.

4.2. Biological evaluation

4.2.1. In vitro studies

4.2.1.1. Anti-inflammatory screening. The synthesized compounds were screened for anti-inflammatory activity by the inhibition of albumin denaturation technique [36].

Diclofenac sodium (standard drug) and test compounds were dissolved in minimum amount of DMF and diluted with phosphate buffer saline (pH 7.4) in such a way that concentration of DMF in all solutions was less than 2.5%. Test solutions (1 cm^3, 100 μg/cm^3) were mixed with 1 cm^3 of 1% albumin solution in phosphate buffer saline and incubated at 27 ± 1 °C in an incubator for 15 min. Denaturation was induced by keeping the reaction mixture at 60 ± 1 °C in a water bath for 10 min. After cooling, the turbidity was measured at 660 nm with UV–Visible spectrophotometer. Percentage inhibition of denaturation was then calculated from control where no drug was added. Each experiment was done in triplicate and average taken. The percentage of inhibition was calculated using the formula:

$$\% \text{ Inhibition of denaturation} = [(Vt/Vc) - 1] \times 100$$

where Vt = mean absorption of test compound, Vc = mean absorption of control.

4.2.1.2. Antioxidant assay. All the compounds were evaluated *in vitro* for their 2,2′-diphenyl-1-picrylhydrazyl (DPPH) radical scavenging potential as described earlier [37]. Stock solutions of different compounds (1 mM) were mixed with DPPH methanol solution (0.5 cm^3, 0.3 mM) in 3 cm^3 of total reaction mixture and allowed to react at room temperature. After 30 min, absorbance was measured at 520 nm and converted to % antioxidant activity. For a comparative study BHA was used as the standard. The percentage inhibition activity was calculated by using the formula:

$$\% \text{ Activity} = [1 - \text{absorbance of test compound} / \text{absorbance of control compound}] \times 100$$

4.2.1.3. p38α MAP kinase assay. p38α MAP kinase assay was performed using the CycLex p38 Kinase assay kit (Cat# CY-1177) procured from Medical and Biological Laboratories International Corporation (MBLI), Boston, USA. CycLex p38α positive control (Cat# CY-E1177) was also purchased from MBLI, USA. Inhibition of p38α MAP kinase activity was determined according to the method of Forrer *et al* [38].

4.2.2. In vivo studies

Twelve-week old adult male/female Wistar rats (150–200 g) and Balb/c mice (20–30 g) used in the present study were housed and kept in accordance with the Jamia Hamdard Animal Care Unit, which applies the guidelines and rules laid down by Committee for the purpose of control and supervision of Experiments on Animals (173/GO/Re/S/2000/CPCSEA), Ministry of Social Justice and Empowerment, Government of India. Animals were housed in a ventilated room at 25 ± 2 °C under a 12 h light/dark cycle in large spacious polypropylene cages. Animal facilities and other areas in contact with laboratory animals were cleaned and disinfected. Animals were allowed to acclimatize for one week before the study and had free access to standard laboratory feed and water *ad libitum*.

4.2.2.1. Anti-inflammatory activity. The synthesized compounds were evaluated for their anti-inflammatory activity using carrageenan induced rat hind paw edema method [39]. The animals were randomly allocated into groups of six animals each and fasted for 24 h before the experiment with free access to water. Control group received only 0.5% CMC solution. Standard, diclofenac sodium was administered orally at a dose of 10 mg/kg. The test compounds were administered orally at an equimolar oral dose relative to 10 mg/kg diclofenac sodium. 0.1 cm^3 of 1% carrageenan solution in saline was injected subcutaneously into the sub plantar region of the right hind paw of each rat, 1 h after the administration of the test compounds and standard drug. The right hind paw volume was measured before and after 4 h of carrageenan treatment by means of a plethysmometer. The percent edema inhibition was calculated from the mean effect in the control and treated animals according to the following equation:

$$\text{Percent edema inhibition} = (V_c - V_t/V_c) \times 100$$

where V_t represents the mean increase in paw volume in rats treated with test compounds and V_c represents the mean increase in paw volume in control group of rats.

For the ulcerogenic activity the same group of rats which were used for anti-inflammatory activity were used after a washout period of 15 days.

4.2.2.2. Ulcerogenic activity. The ulcerogenic effect of five active compounds and diclofenac sodium was evaluated by the reported

method [40]. The rats were allocated into different groups consisting of six animals in each group. Ulcerogenic activity was evaluated after oral administration of the test compounds at an equimolar dose relative to 30 mg/kg diclofenac sodium. Control group received only 0.5% carboxymethylcellulose (CMC) solution. Food but not water was stopped 24 h before administration of the test compounds. After the drug treatment, the rats were fed with normal diet for 17 h and then sacrificed. The stomach was removed and opened along the greater curvature, washed with distilled water and cleaned gently by dipping in normal saline. The mucosal damage was examined by means of a magnifying glass. For each stomach the mucosal damage was assessed according to the following scoring system:

0.5: redness, 1.0: spot ulcers, 1.5: hemorrhagic streaks, 2.0: ulcers > 3 but ≤ 5, 3.0: ulcers > 5. The mean score of each treated group minus the mean score of control group was regarded as severity index of gastric mucosal damage.

4.2.2.3. Lipid peroxidation. Lipid peroxidation in the gastric mucosa was determined according to the method of Ohkawa et al. [41]. After screening the stomach for ulcers the gastric mucosa of glandular portion was scrapped with the help of two glass slides. Gastric mucosa was weighed (100 mg) and homogenized in mortar and pestle with 1.8 cm^3 ice cold 1.15% KCl solution. The homogenate supplemented with 0.2 cm^3 of 8.1% Sodium dodecyl sulphate (SDS), 1.5 cm^3 of acetate buffer and 1.5 cm^3 of 0.8% thiobarbituric acid. The mixture was then incubated at 95 °C for 60 mins on boiling water bath. The reaction mixture was kept at room temperature for some time and then extracted with a mixture of *n*-butanol: pyridine (15: 1, v/v; 5 cm^3) by shaking vigorously for 1 min and then keeping in ice for 2 mins. The organic layer was centrifuged at 3000 rpm for 10 mins. Organic layer was separated out and absorbance measured at 532 nm on UV spectrophotometer. Results were expressed as nmol MDA/100 mg tissue using extinction coefficient $1.56 \times 10^5\ cm^{-1}\ M^{-1}$. Concentration = (Absorbance × volume × 10^9) ÷ ($1.56 \times 10^5 \times 1000$).

4.2.2.4. Determination of the inhibition of LPS-induced TNF-α production. The commercially available ELISA kit (Cat# KB2052, Krishgen Biosystems, Mumbai, India) was used for TNF-α estimation in the mice plasma samples. Lipopolysaccharide (LPS) from E.Coli 0111:B4 (Cat# 9028) was obtained from Chondrex, USA. TNF-α production inhibition in mice (Balb/c) weighing 20–30 g was carried out by the already reported procedure [42,43]. Mice were deprived of food overnight, but not water. The next day, these mice were orally administered with test compounds at an equimolar oral dose relative to 30 mg/kg SB 203580 inhibitor suspended in 0.5% CMC aqueous solution at 10 cm^3/kg. The groups of normal and control mice were administered only with 0.5% CMC aqueous solution at 10 cm^3/kg. Thirty minutes later, LPS solution dissolved in physiological saline was intravenously injected at 0.45 mg/10 cm^3/kg except for the group of normal mice, which were injected with physiological saline at 10 cm^3/kg. One hour later, blood samples were taken from the mice from the vena cava inferior into a syringe containing heparin sodium. After centrifugation of the blood samples at 13,230*g* for 3 mins at 4 °C, plasma samples were taken immediately and frozen at −20 °C until measurement of the concentration of TNF-α. The concentrations of TNF-α in the plasma samples were measured with commercially available ELISA kit. The percent inhibition of TNF-α production was obtained by the following equation: Percent inhibition = {1 − (concentration of TNF-α in plasma sample of mice administrated test compounds − mean concentration of TNF-α in the plasma samples of normal mice)/(concentration of TNF-α in the plasma samples in control mice − mean concentration of TNF-α in the plasma samples of normal mice)} × 100.

4.3. Docking studies

Docking studies of compounds 6a-i against enzyme p38 α MAPK was performed on Maestro 11.2 software installed on Lenovo 30B4A21900 workstation having Intel(R) Xeon(R) CPU E5-2620 v3 @ 2.40 GHz Processor, Windows 7 Operating System; 16 GB RAM; and 4 GB NVIDIA Quadro K620 graphics card. The ligands 6a-i were submitted for preparation to LigPrep module of Maestro for ligand preparation, where the ligands were prepared using OPLS_2005 force-field, at target pH 7.0 ± 2.0 using Epik. The X-ray crystal structure of the protein p38 α MAPK (2LGC) was downloaded from protein data bank (http://www.rcsb.org/pdb). The protein was prepared in protein preparation wizard of Maestro, in which its structure was pre-processed, optimized and minimization using force-field OPLS 2005. Receptor grid was generated next by selecting the active site residues. The co-ordinates of the prepared grid were: x = 11.42, y = 14.62, z = -29.7. Validation of the docking protocol was done by calculating enrichment factor for which known p38 α MAPK inhibitors (22) were merged with decoy set containing 1000 molecules, docking was performed, ROC curve and BEDROC calculations were carried out. The prepared ligands were docked against generated grid using Glide module of maestro using extra precision mode (XP).

Acknowledgements

The authors are thankful to In-charge animal house (for providing animals) and In-charge, Central Instrumentation Facility (CIF) (for spectral analysis of compounds) of School of Pharmaceutical Education and Research, Jamia Hamdard. The author (Kanagasabai Somakala) is thankful to Department of Science and Technology Women Scientists Scheme – A (File No.: SR/WOS-A/CS-84/2013), New Delhi for providing financial assistance.

Conflict of interest

The authors have declared on conflict of interest.

References

[1] G. Singh, G. Triadafilopoulos, Epidemiology of NSAID induced gastrointestinal complications, J. Rheumatol. Suppl. 56 (1999) 18–24.
[2] C.J. Smith, Y. Zhang, C.M. Koboldt, J. Muhammad, B.S. Zwefel, A. Shaffer, J.J. Talley, J.L. Masferrer, K. Serbert, P.C. Isakson, Pharmacological analysis of cyclooxygenase-1 in inflammation, Proc. Natl. Acad. Sci. USA 95 (1998) 13313–13318.
[3] G. Dannhardt, W. Kiefer, Cyclooxygenase inhibitors-current status and future prospects, Eur. J. Med. Chem. 36 (2001) 109–126.
[4] C. Almansa, J. Alfon, A.D. Arriba, F. Cavalcanti, I. Escamilla, L. Gomez, A. Miralles, R. Soliva, J. Bartolli, E. Carceller, M. Merlos, J. Garcia-Rafanell, Synthesis and structure-activity relationship of a new series of COX-2 selective inhibitors: 1,5-diarylimidazoles, J. Med. Chem. 46 (2003) 3463–3475.
[5] U. Salgin-Goksen, N. Gokhan-Kelekci, O. Goktas, Y. Koysal, E. Kilic, S. Isik, G. Aktay, M. Ozalp, 1-Acylthiosemicarbazides, 1,2,4-triazole-5(4H)-thiones, 1,3,4-thiadiazoles and hydrazones containing 5-methyl-2-benzoxazolinones: synthesis, analgesic-anti-inflammatory and antimicrobial activities, Bioorg. Med. Chem. 15 (2007) 5738–5751.
[6] J.J. Talley, D.L. Brown, J.S. Carter, M.J. Graneto, C.M. Koboldt, J.L. Masferrer, W.E. Perkins, R.S. Rogers, A.F. Shaffer, Y.Y. Zhang, B.S. Zweifel, K. Seibert, 4-[5-Methyl-3-phenylisoxazol-4-yl]-benzenesulfonamide, Valdecoxib: A potent and selective inhibitor of COX-2, J. Med. Chem. 43 (2000) 775–777.
[7] K. Brune, B. Hinz, Selective cyclooxygenase-2 inhibitors: similarities and differences, Scand. J. Rheumatol. 33 (2004) 1–6.
[8] D.O. Stichtenoth, J.C. Freolich, The second generation of COX-2 inhibitors: what advantages do the newest offer? Drugs 63 (2003) 33–45.
[9] I.W. Moreland, M.H. Schiff, S.W. Baumgartner, E.A. Tindall, R.M. Fleischmann, K.J. Bulpitt, A.L. Weaver, Etanercept therapy in rheumatoid arthritis. A randomized, controlled trial, Ann. Int. Med. 130 (1999) 478–486.
[10] M.E. Weinblatt, E.C. Keystone, D.E. Furst, L.M. Moreland, M.H. Weisma, C.A. Birbara, L.A. Teoh, S.A. Fischkoff, E.K. Chartash, Adalimimab, a fully human anti-tumour necrosis factor α monoclonal antibody, for the treatment of rheumatoid arthritis in patients taking concomitant methotrexate: The ARMADA trial, Arth. Rheumat. 48 (2003) 35–45.
[11] R. Maini, E.W. St Clair, F. Breedveld, D. Furst, J. Kalden, M. Weisman, J. Smolen, P. Emery, G. Harriman, Infliximab (chimeric anti-tumour necrosis factor α

monoclonal antibody) versus placebo in rheumatoid arthritis patients receiving concomitant methotrexate: a randomized phase III trial. Attract study group, Lancet 354 (1999) 1932–1939.
[12] C. Yazdani, T. McLaughlin, G. Cummins, J. Doyle, Comparison of rheumatoid arthritis care costs in patients starting therapy with leflunomide versus etanercept, Am. J. Manage. Care 7 (2001) S419–S426.
[13] (a) S. Margutti, S.A. Laufer, Are MAP kinases drug targets? Yes but difficult ones, Chem. Med. Chem. 2 (2007) 1116–1140;
(b) G. Schett, J. Zwerina, G. Firestein, The p38 mitogen-activated protein kinase (MAPK) pathway in rheumatoid arthritis, Ann. Rheum. Dis. 67 (2008) 909–916.
[14] S.J. O'Keefe, J.S. Mudgett, S. Cupo, J.N. Parsons, N.A. Chartrain, C. Fitzgerald, S.L. Chen, K. Lowitz, C. Rasa, D. Visco, S. Luell, E. Carballo-Jane, K. Owens, D.M. Zaller, Chemical genetics define the roles of p38α and p38β in acute and chronic inflammation, J. Biol. Chem. 282 (2007) 34663–34671.
[15] (a) L.H. Pettus, R.P. Wurz, Small molecule p38 MAP kinase inhibitors for the treatment of inflammatory diseases: novel structures and developments during 2006–2008, Curr. Top. Med. Chem. 8 (2008) 1452–1467;
(b) G. Wagner, S. Laufer, Small molecular anti-cytokine agents, Med. Res. Rev. 26 (2006) 1–62;
(c) J. Westra, P.C. Limburg, p38 mitogen activated protein kinase (MAPK) in rheumatoid arthritis, Mini Rev. Med. Chem. 6 (2006) 867–874;
(d) C. Dominguez, N. Tamayo, D. Zhang, p38 inhibitors: beyond pyridinylimidazoles, Exp. Opin. Ther. Pat. 15 (2005) 801–816;
(e) C. Dominguez, D.A. Powers, N. Tamayo, p38 MAP kinase inhibitors: many are made but few are chosen, Curr. Opin. Drug Dis. Dev. 8 (2005) 421–430.
[16] M.R. Gola, V.M. Barota, Facile multi-components one-pot synthesis of dipyrazolo [1,5-*a*:3',4'-*d*]pyrimidine as potent bioactive scaffolds, Curr. Chem. Lett. 7 (2018) 111–120.
[17] Y.Y. Wang, F.Z. Xu, B. Song, D. Luo, G. Yu, S. Chen, W. Xue, J. Wu, Pyrazolo[3,4-*d*] pyrimidine derivatives containing a Schiff base moiety as potential antiviral agents, Bioorg. Med. Chem. Lett. 28 (2018) 2979–2984.
[18] G.N. Tageldin, S.M. Fahmy, H.M. Ashour, M.A. Khalil, R.A. Nassra, I.M. Labouta, Design, synthesis and evaluation of some pyrazolo[3,4-*d*]pyrimidines as anti-inflammatory agents, Bioorg. Chem. 78 (2018) 358–371.
[19] G.N. Tageldin, S.M. Fahmy, H.M. Ashour, M.A. Khalil, R.A. Nassra, I.M. Labouta, Design, synthesis and evaluation of some pyrazolo[3,4-*d*]pyrimidine derivatives bearing thiazolidinone moiety as anti-inflammatory agents, Bioorg. Chem. 80 (2018) 164–173.
[20] M. Maher, A.E. Kassab, A.F. Zaher, Z. Mahmoud, Novel pyrazolo[3,4-*d*]pyrimidines: design, synthesis, anticancer activity, dual EGFR/ErbB2 receptor tyrosine kinases inhibitory activity, effects on cell cycle profile and caspase-3-mediated apoptosis, J. Enz. Inhib. Med. Chem. 34 (2019) 532–546.
[21] M. Allam, A.K.D. Bhavani, A. Mudiraj, N. Ranjan, M. Thippana, P.P. Babu, Synthesis of pyrazolo[3,4-*d*]pyrimidin-4(5*H*)-ones tethered to 1,2,3-triazoles and their evaluation as potential anticancer agents, Eur. J. Med. Chem. 156 (2018) 43–52.
[22] A.A. Gaber, A.H. Bayoumi, A.M. El-morsy, F.F. Sherbiny, A.B.M. Mehany, I.H. Eissa, Design, synthesis and anticancer evaluation of 1*H*-pyrazolo[3,4-*d*]pyrimidine derivatives as potent $EGFR^{WT}$ and $EGFR^{T790M}$ inhibitors and apoptosis inducers, Bioorg. Chem. 80 (2018) 375–395.
[23] L. Revesz, E. Blum, F.E. Di Padova, T. Buhl, R. Feifel, H. Gram, P. Hiestand, U. Manning, U. Neumann, G. Rucklin, Pyrazoloheteroaryls: novel p38α MAP kinase inhibiting scaffolds with oral activity, Bioorg. Med. Chem. Lett. 16 (2006) 262–266.
[24] J. Das, R.V. Moquin, S. Pitt, R. Zhang, D.R. Shen, K.W. McIntyre, K. Gillooly, A.M. Doweyko, J.S. Sack, H. Zhang, S.E. Kiefer, K. Kish, M. McKinnon, J.C. Barrish, J.H. Dodd, G.L. Schieven, K. Leftheris, Pyrazolo-pyrimidines: a novel heterocyclic scaffold for potent and selective p38 alpha inhibitors, Bioorg. Med. Chem. Lett. 18 (2008) 2652–2657.
[25] M. Soth, S. Abbot, A. Abubakari, N. Arora, H. Arzeno, R. Billedeau, N. Dewdney, K. Durkin, S. Frauchiger, M. Ghate, D.M. Goldstein, R.J. Hill, A. Kuglstatter, F. Li, B. Loe, K. McCaleb, J. McIntosh, E. Papp, J. Park, M. Stahl, R. Man-Ling Sung, D.C. Suttman, P. Swinney, B. Weller, H. Wong, T. Gabriel Zecic, 3-Amino-pyrazolo [3,4-d]pyrimidines as p38α kinase inhibitors: design and development to a highly selective lead, Bioorg. Med. Chem. Lett. 21 (2011) 3452–3456.
[26] N.S.M. Ismail, E.M.H. Ali, D.A. Ibrahim, R.A.T. Serya, D.A. Abou El Ella, Pyrazolo [3,4-d]pyrimidine based scaffold derivatives targeting kinases as anticancer agents, Fut. J. Pharma. Sci. 2 (2016) 20–30.
[27] M. Amir, K. Somakala, S. Ali, p38 MAP kinase as anti-inflammatory agents, Min. Rev. Med. Chem. 13 (2013) 2082–2096.
[28] K. Somakala, M. Amir, V. Sharma, S. Wakode, Synthesis and pharmacological evaluation of pyrazole derivatives containing sulfonamide moiety, Monatsh. Chem. 147 (2016) 2017–2029.
[29] K. Somakala, M. Amir, Synthesis characterization and pharmacological evaluation of pyrazolyl urea derivatives as potential anti-inflammatory agents, Act. Pharma. Sinic.-B 7 (2) (2017) 230–240.
[30] S. Tariq, O. Alam, M. Amir, Synthesis, anti-inflammatory, p38a MAP kinase inhibitory activities and molecular docking studies of quinoxaline derivatives containing triazole moiety, Bioorg. Chem. 76 (2018) 343–358.
[31] S. Tariq, P. Kamboj, O. Alam, M. Amir, 1,2,4-Triazole-based benzothiazole/benzoxazole derivatives: design, synthesis, p38α MAP kinase inhibition, anti-inflammatory activity and molecular docking studies, Bioorg. Chem. 81 (2018) 630–641.
[32] S. Tariq, O. Alam, M. Amir, Synthesis, p38α MAP kinase inhibition, anti-inflammatory activity, and molecular docking studies of 1,2,4-triazole-based benzothiazole-2-amines, Arch. Pharm. Chem. Life Sci. 351 (2018) e1700304.
[33] A.H. Abdelazeem, S.A. Abdelatef, M.T. El-Saadi, H.A. Omar, S.I. Khan, C.R. McCurdy, S.M. El-Moghazy, Novel pyrazolopyrimidine derivatives targeting COXs and iNOS enzymes; design, synthesis and biological evaluation as potential anti-inflammatory agents, Eur. J. Pharm. Sci. 62 (2014) 197–211.
[34] J. Sheehan, P.A. Cruickshank, Notes-A convenient synthesis of water-soluble carbodiimides, J. Org. Chem. 26 (1961) 2525–2528.
[35] G.C. Windridge, E.C. Jorgensen, 1-Hydroxybenzotriazole as a racemization-suppressing reagent for the incorporation of im-benzyl-L-histidine into peptides, J. Am. Chem. Soc. 17 (1971) 6318–6319.
[36] Y. Mizushima, M.J. Kobayashi, Interaction of anti-inflammatory drugs with serum proteins, especially with some biologically active proteins, Pharm. Pharmacol. 20 (1968) 169–173.
[37] M.S. Blois, Antioxidant determination by the use of a stable free radical, Nature 181 (1958) 1119–1200.
[38] P. Forrer, R. Tamaskovic, R. Jaussi, Enzyme-linked immunosorbent assay for measurement of JNK, ERK, and p38 kinase activities, Biol. Chem. 379 (1998) 1101–1111.
[39] C.A. Winter, E.A. Risely, G.M. Nuss, Carrageenen-induced edema in hind paw of the rat as an assay for antiiflammatory drugs, Proc. Soc. Exp. Biol. Med. 111 (1962) 544–547.
[40] V. Cioli, S. Putzolu, V. Rossi, P. Sorza Barcellona, C. Corradino, The role of direct tissue contact in the production of gastro-intestinal ulcer by anti-inflammatory drugs in rats, Toxicol. Appl. Pharmacol. 50 (1979) 283–289.
[41] H. Ohkawa, N. Ohishi, K. Yagi, Assay for lipid peroxides in animal tissues by thiobarbituric acid reaction, Anal. Biochem. 95 (1979) 351–358.
[42] D.E. Griswold, L.M. Hilegass, L. O'Leary-Bartus, J.C. Lee, J.T. Laydon, T.J. Trophy, Evaluation of human cytokine production and effects of pharmacological agents in a heterologous system *in vivo*, J. Immunol. Methods. 195 (1996) 1–5.
[43] A. Nakao, N. Ohkawa, T. Nagasaki, T. Kagari, H. Doi, T. Shimozato, S. Ushiyama, K. Aoki, Tetrahydropyridine derivatives with inhibitory activity on the production of proinflammatory cytokines: part 1, Bioorg. Med. Chem. Lett. 19 (2009) 4607–4610.